



HAL
open science

Pseudo-dihedral Angles in Proteins Providing a New Description of the Ramachandran Map

Wagner da Rocha, Carlile Lavor, Leo Liberti, Thérèse Malliavin

► **To cite this version:**

Wagner da Rocha, Carlile Lavor, Leo Liberti, Thérèse Malliavin. Pseudo-dihedral Angles in Proteins Providing a New Description of the Ramachandran Map. International Conference on Geometric Science of Information, Aug 2023, Saint-Malo, France. pp.511-519, 10.1007/978-3-031-38299-4_53 . hal-04185420

HAL Id: hal-04185420

<https://inria.hal.science/hal-04185420>

Submitted on 22 Aug 2023

HAL is a multi-disciplinary open access archive for the deposit and dissemination of scientific research documents, whether they are published or not. The documents may come from teaching and research institutions in France or abroad, or from public or private research centers.

L'archive ouverte pluridisciplinaire **HAL**, est destinée au dépôt et à la diffusion de documents scientifiques de niveau recherche, publiés ou non, émanant des établissements d'enseignement et de recherche français ou étrangers, des laboratoires publics ou privés.



Distributed under a Creative Commons Attribution 4.0 International License

Pseudo-dihedral angles in proteins providing a new description of the Ramachandran map^{*}

Wagner Da Rocha^{1,2}[0000-0002-3894-4002], Carlile Lavor³[0000-0002-8105-3627], Leo Liberti²[0000-0003-3139-6821], and Thérèse E Malliavin¹[0000-0002-3276-3366]

¹ Laboratoire de Physique et Chimie Théorique, CNRS UMR7019 et Université de Lorraine, France therese.malliavin@univ-lorraine.fr

² Laboratoire d'Informatique de l'École Polytechnique, CNRS UMR 7161, France leo.liberti@polytechnique.edu, wagner.rocha@lix.polytechnique.fr

³ University of Campinas (IMECC - UNICAMP), Brazil clavor@unicamp.br

Abstract. Since the first years of structural biology, the Ramachandran map has provided a simple definition of the curvilinear geometry of the protein backbone. Its definition is mainly based on the values of the dihedral angles ϕ and ψ measured between the heavy atoms of the protein backbone. Discontinuities in angle values are observed, particularly in the region of the β -strand secondary structure. We introduce new pseudo-dihedral angles involving hydrogen positions instead of some of the positions of the heavy atoms. We determine simple relationships between the old and new dihedral angles. We show that combining the old and new parameters allows us to overcome the discontinuity problem encountered in the Ramachandran map.

Keywords: interval Branch-and-Prune · pseudo-dihedral angles · Ramachandran map.

1 Introduction

The development of structural biology has produced the availability of numerous protein structures. These structures can be considered as geometrical objects provided by nature and are therefore the subject of ongoing interest [6,10,15]. A reasonable quantification of the geometry in proteins is essential for a better definition of the biological function and activity of these molecules. The approaches easing this quantification are thus crucial for application-oriented developments in health and biotechnology.

For a decade, the Branch-and-Prune (BP) and interval Branch-and-Prune (*i*BP) algorithms have been developed to provide a solution of the Distance Geometry Problem. These algorithms provide a theoretical framework for the parametrization as well as a systematic enumeration of the atomic coordinates [4,5]. These algorithms are based on the use of known inter-atomic distances as

^{*} Supported by CNPq, FAPESP, UNICAMP, CNRS, École Polytechnique and Université de Lorraine.

well as dihedral angles [14], and the derivation of relationships between angles would enlarge the possible applications. We present here a geometric relationship between the protein backbone dihedral angles ϕ and ψ to pseudo-dihedral angles defined from backbone atoms, including hydrogens (Section 2). Furthermore, we calibrate these formulas experimentally on data from sets of protein structures (Section 3). This new way to observe the curvilinear geometry of the backbone angles allows us to solve a discontinuity problem present in the classical definition of the Ramachandran map [11]. Removing the discontinuity helps to improve the systematic enumeration of protein conformations in the *i*BP algorithm [7] by avoiding the definition of multiple intervals due to the gaps in angle values.

2 Theory

The dihedral (torsion) angles in protein structures are defined for sets of four 3D Cartesian coordinates representing atoms A , B , C and D as the angles between the vectors normal to the planes $\{A, B, C\}$ and $\{B, C, D\}$. Considering two amino acid residues in a protein, consecutive in the primary sequence, R_i and R_{i+1} , the backbone dihedral angles are defined as [9]:

$$\begin{aligned}\phi_i &:= C^{i-1} - N^i - C_\alpha^i - C^i, \\ \psi_i &:= N^i - C_\alpha^i - C^i - N^{i+1}, \\ \omega_i &:= C_\alpha^{i-1} - C^{i-1} - N^i - C_\alpha^i,\end{aligned}\tag{1}$$

where the ω_i angle populates two sets of values: $\omega_i \approx 0^\circ$, in the case of the *cis* peptide bond, or $|\omega| \approx 180^\circ$ in the case of the *trans* peptide bond.

By analogy with the definition from (1), and considering the amino acid residues R_j , R_i , and R_{i+1} , we define the following pseudo-dihedral angles:

$$\begin{aligned}\nu_{ji}^\kappa &:= C^{i-1} - N^i - C_\alpha^i - H_\kappa^j, & v_{ji}^\kappa &:= N^i - C_\alpha^i - C^i - H_\kappa^j, \\ \xi_i &:= H_\rho^i - N^i - C_\alpha^i - C^i, & \zeta_i &:= H_\varrho^{i+1} - C_\alpha^i - C^i - N^{i+1}, \\ \mu_{ji}^\kappa &:= H_\kappa^j - N^i - C_\alpha^i - H_\rho^i, & \eta_{ji}^\kappa &:= H_\kappa^j - C_\alpha^i - C^i - H_\varrho^{i+1},\end{aligned}\tag{2}$$

where $\rho = \begin{cases} \alpha_2 & \text{if } R_i = \text{Glycine}, \\ \alpha & \text{otherwise,} \end{cases}$ $\varrho = \begin{cases} \delta_3 & \text{if } R_{i+1} = \text{Proline}, \\ N & \text{otherwise,} \end{cases}$ and κ represents

any character that names a hydrogen atom in a protein. We need specific notations for the two amino acid residues Glycine and Proline: indeed, in Glycine residues, two hydrogen atoms are bonded to the C_α atom, H_{α_2} and H_{α_3} [9], and we select H_{α_2} to play the role of H_α ; in Proline residues, no H_N atom is present, and we replace the atom H_N by H_{δ_3} .

As the backbone angles are defined in the interval $(-180^\circ, 180^\circ]$, all pseudo-dihedral angles expressed in this paper are also in this interval, and obey the same orientation: the counter-clockwise sense is positive and clockwise sense is negative. Concerning equations (1) and (2), the angles ν_{ji}^κ , ξ_i , and μ_{ji}^κ are

associated to the angle ϕ_i and the others to the angle ψ_i . We note that all angle definitions share the same two central atoms.

We present some examples about pseudo-dihedral angles in a protein structure. If R_i is neither a Proline nor a Glycine amino acid residue, assuming $i = j$, then $\kappa = N$ and $\rho = \alpha$ in the pseudo-dihedral angles defined in (2). To simplify the notation in this case, we consider $\nu_i \equiv \nu_{ii}^N$ and $\mu_i \equiv \mu_{ii}^N$. In Fig. 1, the case where $|\nu_i| \approx 180^\circ$ and $\xi_i \approx -120^\circ$ is presented.

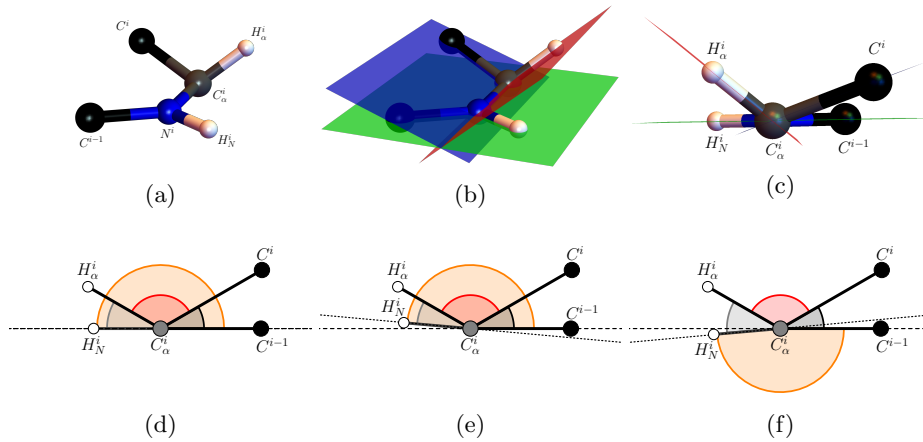


Fig. 1. (a) Spatial positions for the atoms C^{i-1} , N^i , H_N^i , C_α^i , H_α^i , and C^i whether $\nu_i = 180^\circ$, $\xi_i = -120^\circ$, and $\phi_i = 30^\circ$. The numerical values bond length and bond angles are taken from [1]; (b) Definition of the planes $\{C^{i-1}, N^i, C_\alpha^i\}$ (green), $\{N^i, C_\alpha^i, C^i\}$ (blue), and $\{N^i, C_\alpha^i, H_\alpha^i\}$ (red) on the image (a) structure; (c) Rotation of image (b) structure identifying a pertinent point of view; (d) Orthogonal projection of the image (c) structure to the plane perpendicular to the bond $N^i - C_\alpha^i$. The dihedral angle ϕ_i (black) and the pseudo-dihedral angles ν_i (orange), ξ_i (red), and μ_i (light gray) are identified as planar angles and obey the angular relationship: $\phi_i = \nu_i + \xi_i + \mu_i$; (e) Planar approach of image (a) structure concerning $\nu_i = 175^\circ$ with the angular relationship described by $\phi_i = \nu_i + \xi_i + \mu_i$; (f) Analogous case of image (e), though in this case $\nu_i = -175^\circ$ and the angular relationship is expressed by $\phi_i = \nu_i + \xi_i + \mu_i + 360^\circ$.

The dihedral angles are represented in 2D in Fig. 1 (d) to (f) without loss of generality, because we can always define an isometric function to switch the rotation axis defined by atoms N^i and C_α^i to the z -axis of the Cartesian coordinate system [8]. In this case, the angular information required to rotate any point around the z -axis is the same as needed to rotate a point of the plane xy around its origin [8].

The relationship between the dihedral and pseudo-dihedral angles changes depending on the values of the pseudo-dihedral angles involved. Any relationship described from those angles can be considered a composition of rotations in the plane. Indeed, as $\mathbb{R}^2 \cong \mathbb{C}(\mathbb{R})$ [13], we assume without loss of generality that $C_\alpha = 0$ of \mathbb{C} and the atoms C^{i-1} , C^i , H_α^i , and H_N^i are points of \mathbb{C} in a unitary

circle. Then, the following rotations in \mathbb{C} allow the definition of the relative atomic positions:

$$C^i = e^{i\phi_i} C^{i-1}, \quad C^i = e^{i\xi_i} H_\alpha^i, \quad H_\alpha^i = e^{i\mu_i} H_N^i, \quad \text{and} \quad H_N^i = e^{i\nu_i} C^{i-1}, \quad (3)$$

where i is the imaginary unity. From the rotations of (3), we can write:

$$\begin{aligned} e^{i\phi_i} C^{i-1} &= e^{i\xi_i} H_\alpha^i = e^{i\xi_i} e^{i\mu_i} H_N^i = e^{i\xi_i} e^{i\mu_i} e^{i\nu_i} C^{i-1} = e^{i(\xi_i + \mu_i + \nu_i)} C^{i-1} \Leftrightarrow \\ (e^{i\phi_i} - e^{i(\xi_i + \mu_i + \nu_i)}) C^{i-1} &= 0 \Leftrightarrow e^{i\phi_i} = e^{i(\xi_i + \mu_i + \nu_i)}. \end{aligned} \quad (4)$$

The solution for the complex number equation presented in (4) is given by

$$\phi_i = \nu_i + \xi_i + \mu_i + m \times 360^\circ, \quad (5)$$

such that $m \in \mathbb{Z}$. As all angles from (5) lie in the interval $(-180^\circ, 180^\circ]$, only $m \in \{-1, 0, 1\}$ must be considered in this solution.

A similar reasoning can be applied to describe the general case solution, which has pseudo-dihedral angles defined in atoms from the residues R_j , R_i and R_{i+1} , providing the equation (5):

$$\phi_i = \nu_{ji}^\kappa + \xi_i + \mu_{ji}^\kappa + m \times 360^\circ, \quad \text{such that } m \in \{-1, 0, 1\}. \quad (6)$$

For a unique characterization of the result presented in (6), we must specify which value of m has to be considered in each circumstance. Theorem 1 provides a complete analysis.

Theorem 1. *Let R_j and R_i be amino acid residues of a protein, indexed by their positions in the primary sequence; ϕ_i , ν_{ji}^κ , ξ_i , and μ_{ji}^κ be the dihedral and the three pseudo-dihedral angles defined in (1) and (2), respectively. The dihedral angle $\phi_i \in (-180^\circ, 180^\circ]$ can be written in the function of the other three pseudo-dihedral angles by*

$$\phi_i = f_{m(\nu_{ji}^\kappa, \xi_i)}(\lambda_{ji}^\kappa + \mu_{ji}^\kappa), \quad (7)$$

where $\lambda_{ji}^\kappa := \nu_{ji}^\kappa + \xi_i$,

$$m(\theta, \vartheta) := \begin{cases} 1 & \text{if } -180^\circ < \theta \leq -\vartheta, \\ -1 & \text{if } -\vartheta < \theta \leq 180^\circ, \end{cases} \quad (8)$$

and

$$f_m(\tau) := \begin{cases} \tau & \text{if } |\tau| < 180^\circ, \\ \tau + m \times 360^\circ & \text{if } |\tau| > 180^\circ, \\ 180^\circ & \text{if } |\tau| = 180^\circ. \end{cases} \quad (9)$$

Proof. As the pseudo-dihedral angles ν_{ji}^κ and μ_{ji}^κ can assume any value in the interval $(-180^\circ, 180^\circ]$, to analyze all possibilities for these angles, conveniently, we consider the intervals: $\textcircled{i} : -180^\circ < \nu_{ji}^\kappa \leq -\xi_i$ and $\textcircled{ii} : -\xi_i < \nu_{ji}^\kappa \leq 180^\circ$;

① : $-180^\circ < \mu_{ji}^\kappa \leq 0^\circ$ and ② : $0^\circ < \mu_{ji}^\kappa \leq 180^\circ$. As it is mentioned in the examples, $-180^\circ < \xi_i < 0^\circ$; then:

$$\begin{aligned} \textcircled{i} + \textcircled{1} &\Rightarrow -360^\circ < \nu_{ji}^\kappa + \mu_{ji}^\kappa \leq -\xi_i \Leftrightarrow \begin{cases} -360^\circ + \xi_i < \lambda_{ji}^\kappa + \mu_{ji}^\kappa \leq -180^\circ, \\ -180^\circ < \lambda_{ji}^\kappa + \mu_{ji}^\kappa \leq 0^\circ. \end{cases} \\ \textcircled{i} + \textcircled{2} &\Rightarrow \begin{cases} -180^\circ + \xi_i < \lambda_{ji}^\kappa + \mu_{ji}^\kappa \leq -180^\circ, \\ -180^\circ < \lambda_{ji}^\kappa + \mu_{ji}^\kappa \leq 180^\circ. \end{cases} \end{aligned} \quad (10)$$

So, for case \textcircled{i} , we remark:

$$\begin{cases} -360^\circ + \xi_i < \lambda_{ji}^\kappa + \mu_{ji}^\kappa < -180^\circ \\ -180^\circ \leq \lambda_{ji}^\kappa + \mu_{ji}^\kappa \leq 180^\circ \end{cases} \Leftrightarrow \begin{cases} \xi_i < \lambda_{ji}^\kappa + \mu_{ji}^\kappa + 360^\circ < 180^\circ \\ -180^\circ \leq \lambda_{ji}^\kappa + \mu_{ji}^\kappa \leq 180^\circ \end{cases} \quad (11)$$

Observing the result from (11) in (6), we can say:

$$\begin{cases} \phi_i = \lambda_{ji}^\kappa + \mu_{ji}^\kappa + 360^\circ & \text{if } \lambda_{ji}^\kappa + \mu_{ji}^\kappa < -180^\circ, \\ \phi_i = \lambda_{ji}^\kappa + \mu_{ji}^\kappa & \text{if } |\lambda_{ji}^\kappa + \mu_{ji}^\kappa| \leq 180^\circ. \end{cases} \quad (12)$$

With similar arguments from (10), for case \textcircled{ii} , we can write:

$$\begin{cases} \phi_i = \lambda_{ji}^\kappa + \mu_{ji}^\kappa & \text{if } |\lambda_{ji}^\kappa + \mu_{ji}^\kappa| \leq 180^\circ, \\ \phi_i = \lambda_{ji}^\kappa + \mu_{ji}^\kappa - 360^\circ & \text{if } \lambda_{ji}^\kappa + \mu_{ji}^\kappa > 180^\circ. \end{cases} \quad (13)$$

The results from (12) and (13) can be resumed by $\phi_i = f_{m(\nu_{ji}^\kappa, \xi_i)}(\lambda_{ji}^\kappa + \mu_{ji}^\kappa)$ where f_m and m are defined as the theorem presented them.

To determine the relationship among the angles ψ_i , ν_{ji}^κ , ζ_i , and η_{ji}^κ , we can use the same approach as the one shown to derive (6). As in the previous case, this result is given in Theorem 2, which can be proved similarly to Theorem 1.

Theorem 2. *Let R_j , R_i , and R_{i+1} be the amino acid residues of a protein, indexed by their positions in the primary sequence; ψ_i the dihedral angle defined in (1); ν_{ji}^κ , ζ_i , and η_{ji}^κ the pseudo-dihedral angles defined in (2). The dihedral angle $\psi_i \in (-180^\circ, 180^\circ]$ can be written in the function of the other three pseudo-dihedral by*

$$\psi_i = f_{m(\nu_{ji}^\kappa, \zeta_i)}(\sigma_{ji}^\kappa + \eta_{ji}^\kappa), \quad (14)$$

with $\sigma_{ji}^\kappa := \nu_{ji}^\kappa + \zeta_i$, and m and f_m given by (8) and (9), respectively.

In the next section we experimentally provide the numerical expressions proved by the theorems 1 and 2. Our experiments yield the association of the dihedral angles ϕ and ψ with the pseudo-dihedral angles μ and η , respectively, defined in two consecutive amino acid residues of a protein primary sequence. This assumption corresponds to the case $j = i$, and in this frame, the results propose an estimation for the angular constants $\lambda_{ii}^{\kappa_1}$ and $\sigma_{ii}^{\kappa_2}$, with $\kappa_1 \in \{N, \delta_3\}$ and $\kappa_2 \in \{\alpha, \alpha_2\}$.

3 Numerical experiments

A dataset of 226 protein structures was extracted from the list of NMR structures related to the training of the neural network TALOS-N [12], by picking up the first conformer of each structure, as explained in [3].

On the protein structures database, the angles ϕ , ψ , μ , and η are calculated using the python library MDAnalysis [2]. The amino acid residues are sorted into the following types: Glycines, Prolines, and Others. A linear relationship is present by definition between the new angles and the angles ϕ and ψ . In order to explicit these relationship, linear regression was used to determine numerical slopes and intercepts of lines. For each case, at most two lines are observed. Fig. 2 shows the results of the plot $\mu \times \phi$; the regression parameters for this case are presented in Table 1. The numerical calculation of $\eta \times \psi$ is given in Table 2. These numerical results allowed us to determine errors on the slopes and intercepts of the linear relationships presented in the theorems.

The distribution plots of the angles calculated on the database of protein structures are plotted (Fig. 3) using couples of dihedral backbone angles: ϕ/ψ (corresponding to the classical view of Ramachandran plots), μ/η , ϕ/η , and μ/ψ . Depending on the choice of the angle variable, the main secondary structure regions (α -Helix, β -Strand, and Loop) are displaced. For each secondary structure type, there is a combination of angles for which this region is connected in the modified Ramachandran map. This connectedness can simplify the application of the *i*BP algorithm, as the discontinuity due to the periodicity of angle values disappear for the considered secondary structure region.

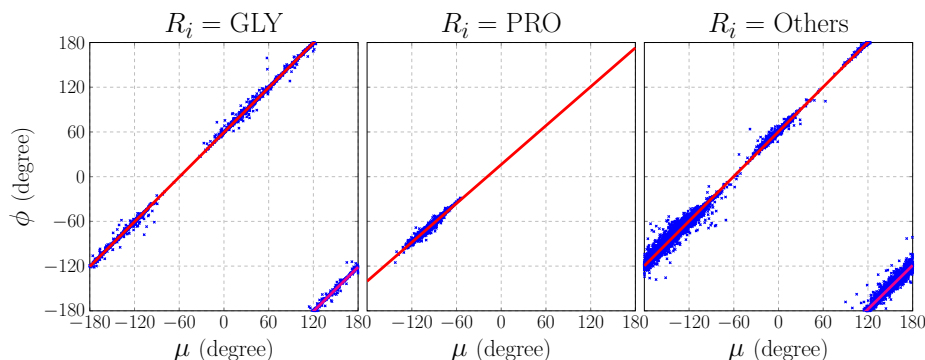


Fig. 2. The data are drawn in blue markers, and its linear regression by continuous lines in red and magenta.

Table 1. Linear Regression Parameters (L.R.P.), slope and intercept values, of the plot $\phi \times \mu$ regarding the equations $\phi_1(\mu) = a_1\mu + a_0$, $\phi_2(\mu) = b_1\mu + b_0$ analyzed on the protein data set.

L.R.P.	GLY	PRO	Others
a_1	1.0003 ± 0.0015	0.8739 ± 0.0137	0.9974 ± 0.0010
a_0	59.4967 ± 0.1477	16.2654 ± 1.3211	60.3836 ± 0.1375
b_1	0.9937 ± 0.0186	—	0.9767 ± 0.0060
b_0	-299.4858 ± 2.7960	—	-295.3706 ± 0.9490

Table 2. Linear Regression Parameters (L.R.P.), slope and intercept values, of the plot $\psi \times \eta$ regarding the equations $\psi_1(\eta) = a_1\eta + a_0$, $\psi_2(\eta) = b_1\eta + b_0$, analyzed on the protein data set.

L.R.P.	$R_i \backslash R_{i+1}$	<i>cis</i> PRO	<i>trans</i> PRO	Others
a_1	GLY	—	0.9900 ± 0.0189	0.9992 ± 0.0013
a_0		—	139.2018 ± 0.8024	120.4346 ± 0.1393
b_1		—	0.9886 ± 0.0170	0.9999 ± 0.0042
b_0		—	-219.8191 ± 1.6198	-239.6703 ± 0.4781
a_1	Others	0.9163 ± 0.0805	1.0011 ± 0.0063	1.0004 ± 0.0003
a_0		81.5530 ± 5.2555	137.6785 ± 0.2224	119.3149 ± 0.0389
b_1		—	0.9896 ± 0.0187	0.9981 ± 0.0026
b_0		—	-221.6108 ± 2.9543	-240.2788 ± 0.3526

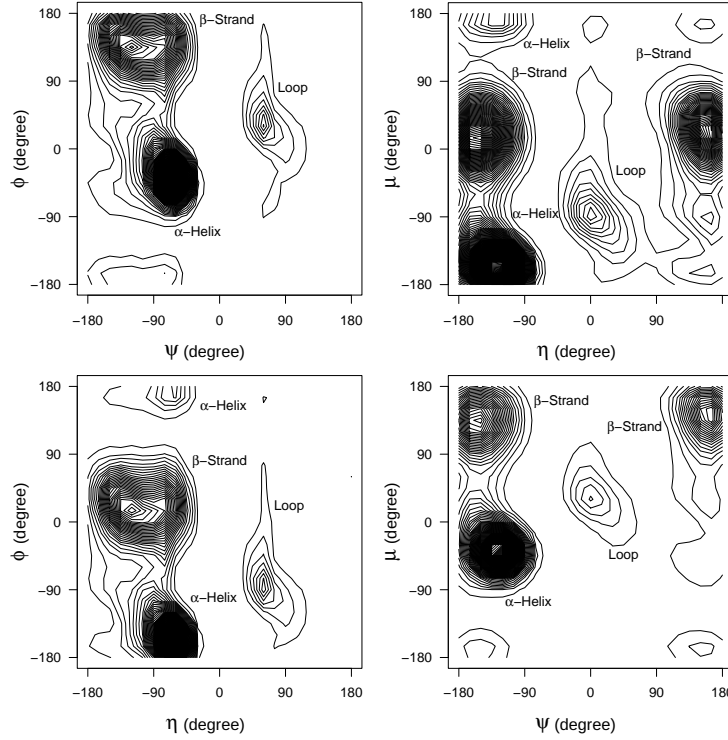


Fig. 3. Distribution of pseudo-dihedral/dihedral \times pseudo-dihedral/dihedral angles. The labels α -Helix, β -Strand, and Loop allow us to follow the displacements of the main secondary structures region on the Ramachandran plot according to the change of variables in angles.

4 Conclusions

The backbone dihedral angles ϕ and ψ were proposed in the 1950s to describe the curvilinear geometry of the protein backbone in the context of the newly developed X-ray crystallography approach for which the hydrogen positions were not visible in protein structures. Among the three main secondary structure regions, the β -Strand spread on regions in which ψ values display discontinuities jumping from 180° to -180° .

Extending the dihedral relationships to angles also involving hydrogen atoms, we proposed here new angles μ and η to describe the curvilinear geometry of the backbone angles. We proved precise relationships between ϕ and μ , and ψ and η . Analyzing the database of protein structures presented above, we obtained numerical values and errors for slopes and intercepts describing the relationships between the angles ϕ , ψ , μ , and η . Combining new and old angles, the discontinuities present in the classical Ramachandran map can be suppressed.

During an *iBP* calculation, the dihedral angle values ϕ and ψ can be used to prune tree branches, or their signed values can be used to create tree branches [14]. In the second case, depending on the considered region of the Ramachandran map, the discontinuities on ϕ and ψ angles can be an obstacle to their straightforward enumeration. In that case, the alternative use of other angle definitions, along with a change of atom ordering, could give the possibility for a straightforward enumeration. A similar approach could be derived, including long-range pseudo-dihedral angles involving atoms located in residues located far apart in the primary protein sequence, and would provide a new point of view on the description of protein structure. Nowadays, most of the long-range are inter-atomic distances, and an angular perspective could bring new insights into protein geometry.

Acknowledgements Ecole Polytechnique, Lorraine University, ANR PRCI “Multi-scale and multi-resolution bio-molecular structure determination by geometric approaches – multiBioStruct” (ANR-19-CE45-0019), CNPq, CNRS, and FAPESP are acknowledged for funding. Wagner Da Rocha thanks the ANR PRCI multiBioStruct (ANR-19-CE45-0019) project for postdoctoral support.

References

1. Engh, R., Huber, R.: Accurate bond and angle parameters for X-ray protein structure refinement. *Acta Crystallogr A* **47**, 392–400 (1991)
2. Gowers, R., Linke, M., Barnoud, J., Reddy, T., Melo, M., Seyler, S., Dotson, D., Domanski, J., Buchoux, S., Kenney, I., Beckstein, O.: MDAnalysis: A Python package for the rapid analysis of molecular dynamics simulations. *Proceedings of the 15th Python in Science Conference, Austin, TX, 2016* **32**, 102–109 (2016)
3. Khalife, S., Malliavin, T., Liberti, L.: Secondary structure assignment of proteins in the absence of sequence information. *Bioinform Adv* **1**(1), vbab038 (2021)

4. Lavor, C., Liberti, L., Mucherino, A.: The interval Branch-and-Prune algorithm for the discretizable molecular distance geometry problem with inexact distances. *J Glob Optim* **56**, 855–871 (2013)
5. Liberti, L., Lavor, C., Maculan, N., Mucherino, A.: Euclidean Distance Geometry and Applications. *SIAM Review* **56**(1), 3–69 (2014)
6. Macari, G., Toti, D., Polticelli, F.: Computational methods and tools for binding site recognition between proteins and small molecules: from classical geometrical approaches to modern machine learning strategies. *J Comput Aided Mol Des* **33**(10), 887–903 (2019)
7. Malliavin, T.E., Mucherino, A., Lavor, C., Liberti, L.: Systematic Exploration of Protein Conformational Space Using a Distance Geometry Approach. *J Chem Inf Model* **59**(10), 4486–4503 (2019)
8. Marsh, D.: *Applied Geometry for Computer Graphics and CAD*. 2nd edn. Springer, London (2005)
9. Nelson, D.L. and Cox, M.M.: *Lehninger Principles of Biochemistry: International Edition*. W.H.Freeman & Co Ltd (2021)
10. Pan, X., Thompson, M.C., Zhang, Y., Liu, L., Fraser, J.S., Kelly, M.J.S., Kortemme, T.: Expanding the space of protein geometries by computational design of de novo fold families. *Science* **369**(6507), 1132–1136 (2020)
11. Ramachandran, G., Ramakrishnan, C., Sasisekharan, V.: Stereochemistry of polypeptide chain configurations. *Journal of Molecular Biology* **7**(1), 95–99 (1963)
12. Shen, Y., Bax, A.: Protein structural information derived from NMR chemical shift with the neural network program TALOS-N. *Methods Mol Biol* **1260**, 17–32 (2015)
13. Suetin, P.K. and Kostrikin, A.I. and Manin, Y.I.: *Linear Algebra and Geometry*. Taylor & Francis (1997)
14. Worley, B., Delhommel, F., Cordier, F., Malliavin, T., Bardiaux, B., Wolff, N., Nilges, M., Lavor, C., Liberti, L.: Tuning interval Branch-and-Prune for protein structure determination. *Journal of Global Optimization* **72**, 109–127 (2018)
15. Zhao, J., Cao, Y., Zhang, L.: Exploring the computational methods for protein-ligand binding site prediction. *Comput Struct Biotechnol J* **18**, 417–426 (2020)